Coronary Calcification and Plaque Vulnerability
An Optical Coherence Tomographic Study

Daniel S. Ong, MD; Jay S. Lee, MS; Tsunenari Soeda, MD, PhD; Takumi Higuma, MD, PhD; Yoshiyasu Minami, MD, PhD; Zhao Wang, PhD; Hang Lee, PhD; Hiroaki Yokoyama, MD, PhD; Takashi Yokota, MD, PhD; Ken Okumura, MD, PhD; Ik-Kyung Jang, MD, PhD

Background—Spotty superficial calcium deposits have been implicated in plaque vulnerability based on previous intravascular imaging studies. Biomechanical models suggest that microcalcifications between 5 and 65 μm in diameter can intensify fibrous cap stress, promoting plaque rupture. However, the 100- to 200-μm resolution of intravascular ultrasound limits its ability to discriminate single calcium deposits from clusters of smaller deposits, and a previous optical coherence tomographic investigation evaluated calcifications within a long segment of artery, which may not truly reflect the mechanics involved in potentiating focal plaque rupture.

Methods and Results—Detailed optical coherence tomographic assessment of coronary calcification at the culprit plaque (10-mm length) was performed in 53 patients with acute ST-segment–elevation myocardial infarction mediated by plaque rupture and 55 patients with stable angina pectoris. The number and longitudinal length of individual calcium deposits were recorded. Cross-sectional images were analyzed every 1 mm for calcium arc and depth, and these quantitative parameters were used to define individual deposits as spotty, large, and superficial. There was no significant difference between ST-segment–elevation myocardial infarction mediated by plaque rupture and stable angina pectoris groups in the number of total (P=0.58), spotty (P=0.87), or large calcium deposits (P=0.27). Minimum calcium depth was similar between groups (P=0.27), as was the number of superficial deposits (P=0.35 using a 65-μm depth threshold and P=0.84 using a 100-μm depth threshold).

Conclusions—The number and pattern of culprit plaque calcifications did not differ between patients presenting with ST-segment–elevation myocardial infarction mediated by plaque rupture versus stable angina pectoris. The optical coherence tomographic assessment of coronary calcification may not be a useful marker of local plaque vulnerability as previously suspected.

Registration Information—URL: http://www.clinicaltrials.gov. Unique identifier: NCT01110538.

(*Circ Cardiovasc Imaging*. 2016;9:e003929. DOI: 10.1161/CIRCIMAGING.115.003929.)

Key Words: atherosclerosis ■ calcium ■ cross-sectional studies ■ myocardial infarction ■ tomography, optical coherence

The effect of coronary artery calcification on local plaque vulnerability remains unclear. The overall degree of coronary calcification, as visualized on angiography and quantified using coronary computed tomography, has been shown to correlate with total atherosclerotic burden and risk of adverse cardiac events.[1,2] However, different patterns in the distribution of coronary artery calcium have been reported to convey different effects on plaque stability. Spotty and superficial calcium deposits have been implicated in plaque vulnerability based on previous intravascular ultrasound (IVUS) studies[3] and 1 optical coherence tomographic (OCT) study.[4] Moreover, biomechanical models suggest that microcalcifications can intensify stress in the fibrous cap, promoting plaque rupture.[5] In contrast, large calcium deposits are hypothesized to promote local biomechanical plaque stability,[6] and statin therapy has been shown to accelerate the calcification of atherosclerotic lesions.[7]

See Editorial by Yahagi et al
See Clinical Perspective

The relatively low resolution of coronary computed tomographic (1 mm) and IVUS (100–200 μm) imaging may limit their ability to discriminate single calcium deposits

Received July 31, 2015; accepted November 20, 2015.

From the Division of Cardiology (D.S.O., J.S.L., T.S., Y.M., Z.W., I.-K.J.) and Biostatistics Center (H.L.), Massachusetts General Hospital, Harvard Medical School, Boston; Department of Cardiology, Hirosaki University Graduate School of Medicine, Hirosaki, Japan (T.H., H.Y., T.Y, K.O.); and Division of Cardiology, Kyung Hee University, Seoul, South Korea (I.-K.J.).

The Data Supplement is available at http://circimaging.ahajournals.org/lookup/suppl/doi:10.1161/CIRCIMAGING.115.003929/-/DC1.

Correspondence to Ik-Kyung Jang, MD, PhD, Cardiology Division, Massachusetts General Hospital GRB 800, 55 Fruit Street, Boston, MA, 02114. E-mail ijang@mgh.harvard.edu

from clusters of multiple smaller deposits. As such, OCT, which has a resolution of 15 to 20 μm, may be a preferred imaging modality for the detailed assessment of coronary calcium.[8] A previous OCT study investigated a potential role for coronary calcifications in plaque vulnerability, identifying a greater prevalence of spotty calcium deposits in patients presenting with acute myocardial infarction (AMI) or unstable angina pectoris (UAP) compared with those presenting with stable angina pectoris (SAP).[4] This OCT investigation, however, evaluated calcifications within a long segment of coronary artery, which may not truly reflect the biomechanics involved in potentiating focal plaque rupture. We, therefore, sought to use OCT to investigate the role of coronary calcium on local plaque vulnerability by performing a detailed assessment of coronary calcification in a limited segment of the culprit artery, comparing the plaques of patients with SAP with those presenting with ST-segment–elevation myocardial infarction mediated by plaque rupture (STEMI-PR).

Methods

Study Population

The STEMI-PR group was extracted from a group of 111 patients who were admitted to Hirosaki University Hospital (Hirosaki, Japan) with STEMI between January 2013 and June 2014, provided written informed consent for the primary percutaneous coronary intervention procedure, and underwent frequency domain OCT imaging of the culprit lesion. STEMI was defined as typical chest pain lasting >20 minutes, ECG showing new ST-segment elevation ≥0.2 mV in at least 2 contiguous precordial leads, ≥0.1 mV in at least 2 contiguous limb leads or new left bundle branch block, and cardiac markers (creatine kinase-MB or cardiac troponin T) elevated above the upper reference limit. Exclusion criteria included cardiogenic shock, unsuccessful reperfusion to achieve antegrade flow despite aspiration thrombectomy, acute stent thrombosis, inability to advance an intravascular imaging catheter to the culprit lesion, and coronary embolism. The culprit lesion was identified on the basis of coronary angiography, electrocardiography, left ventriculography, and echocardiography. Among these 111 patients, we excluded 30 cases of plaque erosion and 9 cases of calcified nodule, resulting in 72 cases with plaque rupture at the culprit site based on OCT imaging. Among these plaque rupture cases, 19 were excluded because of poor image quality, resulting in 53 cases included for final analysis as the STEMI-PR group (Figure I in the Data Supplement).

The Massachusetts General Hospital OCT registry is an international multicenter registry comprised of patients from 20 sites across 6 countries with OCT imaging of the coronary arteries (ClinicalTrials.gov: NCT01110538). We identified 613 patients presenting with SAP in whom frequency domain OCT imaging was performed to the culprit lesion between August 2010 and May 2014. The culprit vessel was identified based on stress testing or as the site with the most severe angiographic stenosis. Among these cases, 536 were excluded because of the lack of preintervention OCT imaging, 14 were excluded because of poor image quality, and 8 were excluded because the culprit frame was located too proximally or distally on pullback imaging to allow full analysis of the 10-mm vessel segment. Finally, 55 cases were included for analysis, comprising the SAP group (Figure II in the Data Supplement). For culprit vessels with serial stenoses, the culprit lesion was identified as that with the smallest minimum luminal area as measured on cross-sectional OCT imaging. The registry was approved by the institutional review board at each participating site, and all patients signed informed consent.

OCT Image Acquisition

A frequency domain OCT system (C7-XR OCT Intravascular Imaging System or ILUMIEN OCT Intravascular Imaging System, St. Jude Medical, Saint Paul, MN) was used in all cases. For the STEMI-PR group, 200 mg aspirin, 300 mg clopidogrel, and 100 IU/kg heparin were administered before the procedure, and manual thrombectomy was performed as needed to restore antegrade coronary flow. The OCT imaging catheter was then advanced distal to the lesion, and automated pullback imaging was performed during simultaneous injection of contrast media or dextran through the guiding catheter to clear blood from the imaging field. Thrombectomy was repeated when image quality was suboptimal. All images were deidentified, digitally stored, and submitted to the Massachusetts General Hospital Cardiac Lab for Integrative Physiology and Imaging for offline analysis using proprietary software (LightLab Imaging).

OCT Image Analysis

OCT image analysis was centered around a designated culprit frame, identified in SAP cases as the cross-sectional image with the minimum lumen area and in STEMI-PR cases as the cross-sectional image at the center of the OCT-identified plaque rupture cavity. In all cases, a 10-mm culprit segment (5 mm proximal to 5 mm distal to the culprit frame) was analyzed. A 30-mm segment (15 mm proximal to 15 mm distal to the culprit frame) was also analyzed in the subset of cases for which these boundaries fell within the 54-mm pullback image length.

Calcium was recognized as heterogeneous areas of high and low reflectivity, with low signal attenuation and a sharply demarcated border. In contrast, lipid was identified as a homogeneous area of low reflectivity with high signal attenuation and a diffuse border. Fibrous tissue was characterized as homogeneous areas of high reflectivity with low signal attenuation.[9] The number and longitudinal length of individual calcium deposits were recorded. Each calcium deposit was categorized as either proximal to, distal to, or spanning the culprit frame. Quantitative analysis was performed using cross-sectional OCT images at 1-mm intervals, and lumen area was measured. Calcium deposits were analyzed individually by measuring calcium arc and depth (minimum distance from lumen to superficial calcium edge). Calcium index was calculated for each calcium deposit as the product of calcium length and mean calcium arc. Total calcium index was calculated as the sum of the calcium index of each calcium deposit within the analyzed vessel segment. The mean calcium index was calculated as the total calcium index divided by the number of calcium deposits. For plaques classified as primarily lipid, the lipid arc and minimum fibrous cap thickness were also recorded.

The spatial relationship between lipid pools and calcium deposits was assessed by measuring the smallest arc separating a calcium deposit from a lipid pool on cross-sectional images. Calcium deposits embedded within, adjacent to, or overlying a lipid pool were considered to have a calcium-to-lipid arc of 0° and termed lipid-interfacing deposits. Spotty calcium deposits (Figure 1A) were defined as those with length <4 mm and maximal arc <90°, and deposits not meeting these criteria were classified as large calcium deposits (Figure 1B).[4,10] Given the lack of established OCT criteria for defining superficial calcium, we used calcium depth thresholds of 65 μm and 100 μm to define individual deposits as superficial-65 and superficial-100, respectively. Calcium deposits were considered distorting if the luminal contour was narrowed or shifted by the shape of the underlying calcium.

Additional plaque characterization was performed according to previously described criteria.[11] Thin-cap fibroatheroma was identified as lipid-rich plaques (lipid arc, >90°) with an overlying minimum fibrous cap thickness of <65 μm. Macrophage accumulations were recognized as linear series of highly reflective (bright) spots with high signal attenuation. Microchannels were defined as signal absent (black) holes within a plaque measuring between 50 and 300 μm in diameter and visible on at least 3 consecutive frames on pullback imaging. Cholesterol crystals were

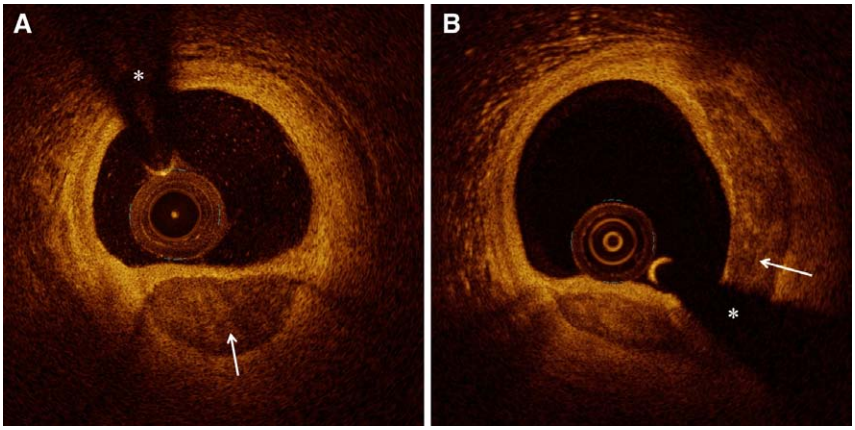

Figure 1. Cross-sectional optical coherence tomography images of calcium. Calcium is identified on optical coherence tomographic images as a heterogeneous area of high and low reflectivity, with low signal attenuation and a sharply demarcated border. **A**, Spotty calcium deposits (arrow) are defined as a deposit with length <4 mm and maximal arc <90°. **B**, Large calcium deposits (arrow) are those with length ≥4 mm or maximal arc ≥90°. The asterisks denote guidewire shadow artifact.

identified as thin linear structures with high reflectivity and low signal attenuation.

Statistical Analysis

Categorical variables are presented as counts and percentages, and comparisons were performed using a Fisher exact or χ^2 test. The distribution of continuous variables was evaluated with the Kolgormonov–Smirnov test. We report mean±SD for normally distributed data and median (25th to 75th percentile) for data that are not normally distributed. Comparisons for continuous variables were performed using an independent samples *t* test or Mann–Whitney *U* test. All tests were 2-sided, and *P* values below a threshold of 0.05 were considered to be significant. All statistical analyses were performed using IBM SPSS Statistics 19.0 (SPSS Inc, Chicago, IL).

Results

Patient Characteristics

A total of 108 plaques were analyzed, including the culprit coronary segments of 55 patients who presented with SAP and 53 patients who presented with STEMI caused by plaque rupture. Baseline demographic and clinical characteristics are summarized and compared as shown in Table 1. Patients in the STEMI-PR group were older and more commonly active smokers than patients in the SAP group. On initial presentation, patients with STEMI-PR were less frequently on aspirin, clopidogrel, β-blockers, or statins than patients with SAP and had higher total cholesterol and low-density lipoprotein levels.

Plaque Characteristics

Quantitative and qualitative plaque characteristics are summarized and compared as shown in Table 2. The minimum luminal area was smaller in the STEMI-PR group compared with the SAP group (1.69±0.73 versus 2.44±1.43 mm^2; *P*<0.01). Culprit plaques in the STEMI-PR group had larger mean lipid arcs (240.2±66.2° versus 146.3±76.5°; *P*<0.01) and thinner fibrous caps (68.8±20.9 versus 123.1±55.6 μm; *P*<0.01) and were more frequently categorized as thin-cap fibroatheroma (56.6% versus 18.2%; *P*<0.01), compared with the culprit plaques in the SAP group. The prevalence of microchannels and macrophages was similar between groups, although cholesterol crystals were more frequently seen in the STEMI-PR group compared with the SAP group (77.4% versus 41.8%; *P*<0.01).

Calcium Analysis

Detailed OCT analysis of calcium deposits is summarized in Table 3. There was no significant difference between the STEMI-PR and SAP groups in the median number of total

Table 1. Patient Characteristics

	STEMI-PR (n=53)	SAP (n=55)	*P* Value
Age, y	69.5±13.1	63.4±10.0	<0.01
Male sex (%)	38 (71.7)	43 (78.2)	0.51
BMI, kg/m^2	24.6±3.64	25.9±4.16	0.07
Risk factors, %			
Hypertension	38 (71.7)	46 (83.6)	0.17
Hyperlipidemia	38 (71.7)	35 (66.0)	0.68
Current smoking	20 (37.7)	8 (15.4)	0.02
Diabetes mellitus	23 (43.4)	14 (25.5)	0.07
Previous MI	2 (3.8)	9 (16.7)	0.05
Medications, %			
Aspirin	5 (9.4)	42 (76.4)	<0.01
Clopidogrel	1 (1.9)	24 (43.6)	<0.01
Statin	11 (22.0)	29 (52.7)	<0.01
β-blocker	3 (6.0)	26 (47.3)	<0.01
ACEi/ARB	16 (30.2)	27 (49.1)	0.05
Labwork, mg/dL			
Creatinine	0.88±0.2	0.94±0.73	0.54
Total cholesterol	201.5±41.0	161.0±39.3	<0.01
LDL	128.8±41.4	91.0±32.9	<0.01
HDL	44.8±10.4	45.4±16.9	0.85
Triglycerides	139.4±137.2	127.8±59.4	0.60

Data are presented as mean±SD or n (%). ACEi indicates angiotensin-converting enzyme inhibitor; ARB, angiotensin receptor blocker; BMI, body mass index; HDL, high-density lipoprotein; LDL, low-density lipoprotein; MI, myocardial infarction; SAP, stable angina pectoris; and STEMI-PR, ST-segment–elevation myocardial infarction plaque rupture.

Table 2. Plaque Characteristics

	STEMI-PR (n=53)	SAP (n=55)	*P* Value
Minimum luminal area, mm^2	1.69±0.73	2.44±1.43	<0.01
Mean lipid arc, °	240.2±66.2	146.3±76.5	<0.01
Minimum FCT, μm	68.8±20.9	123.1±55.6	<0.01
TCFA (%)	30 (56.6)	10 (18.2)	<0.01
Macrophages (%)	50 (94.3)	45 (81.8)	0.07
Microchannels (%)	17 (32.1)	20 (36.4)	0.69
Cholesterol crystals (%)	41 (77.4)	23 (41.8)	<0.01

Data are presented as mean±SD or n (%). FCT indicates fibrous cap thickness; SAP, stable angina pectoris; STEMI-PR, ST-segment–elevation myocardial infarction plaque rupture; and TCFA, thin-cap fibroatheroma.

calcium deposits (*P*=0.58), spotty calcium deposits (*P*=0.87), or large calcium deposits (*P*=0.27). The total calcium index and mean calcium index were also similar between groups (*P*=0.31 and *P*=0.11, respectively).

There was no significant difference in the minimum calcium depth (*P*=0.27), the number of superficial-65 deposits (*P*=0.35), or the number of superficial-100 deposits (*P*=0.84) between the STEMI-PR and SAP groups. Moreover, the number of calcium deposits that were both spotty and superficial-65 or both spotty and superficial-100 was also similar between the STEMI-PR and SAP groups (*P*=0.96 and *P*=0.71, respectively). The number of lipid-interfacing calcium deposits was similar between the STEMI-PR and SAP groups (*P*=0.65). There was also no significant difference in the number of lipid-interfacing calcium deposits that were also spotty (*P*=0.28), spotty and superficial-65 (*P*=0.26), or spotty and superficial-100 (*P*=0.21).

The numbers of calcifications proximal and distal to the culprit frame were similar between the STEMI-PR and SAP groups (*P*=0.44 and *P*=0.45, respectively). However, there was a trend toward a greater number of calcifications spanning the culprit frame in the SAP group compared with the STEMI-PR group (*P*=0.07), and the median number of calcium deposits distorting the lumen was significantly greater in the SAP group compared with the STEMI-PR group (*P*=0.01).

Thirty-Millimeter Segment Analysis

Among the 108 cases included in this study, 70 cases (36 STEMI-PR and 34 SAP) had OCT imaging that enabled analysis of calcifications within a 30-mm segment (from 15 mm proximal to 15 mm distal) spanning the culprit frame. Detailed 30-mm segment OCT analysis of calcium deposits in this subgroup of patients is summarized in Table 4. There was a trend toward a higher number of total calcium deposits (*P*=0.08) and spotty calcium deposits (*P*=0.06) in the STEMI-PR group compared with the SAP group, although this did not reach statistical significance. There was no difference between groups in the number of deposits that were classified as large (*P*=0.66), superficial-65 (*P*=0.60), superficial-100 (*P*=0.42), both spotty and superficial-65 (*P*=0.72), or both spotty and superficial-100 (*P*=0.59).

Discussion

Extracellular calcium deposits have long been recognized as a prominent feature in the development and progression of atherosclerosis.[12] Coronary artery calcification is associated with advanced atherosclerosis[1] and increased risk of adverse cardiac events.[2] However, the specific effect of calcium deposits

Table 3. Optical Coherence Tomography Calcium Analysis

	STEMI-PR (n=53)	SAP (n=55)	*P* Value
Total calcium deposits	1 (0–2.5)	1 (0–3)	0.58
Spotty calcium	1 (0–2)	1 (0–2)	0.87
Large calcium	0 (0–1)	0 (0–1)	0.27
Total calcium index	242.3±282.6	317.1±324.5	0.31
Mean calcium index	92.8±96.1	146.9±173.7	0.11
Minimum calcium depth, μm	111.5±97.1	84.7±103.0	0.27
Superficial-65	0 (0–1)	0 (0–1)	0.35
Superficial-100	0 (0–1)	0 (0–1)	0.84
Spotty and superficial-65	0 (0–0)	0 (0–0)	0.96
Spotty and superficial-100	1 (0–1)	0 (0–1)	0.71
Lipid interfacing	1 (0–2)	1 (0–2)	0.65
Lipid interfacing and spotty	1 (0–1)	0 (0–1)	0.28
Lipid interfacing and spotty and superficial-65	0 (0–0)	0 (0–0)	0.26
Lipid interfacing and spotty and superficial-100	0 (0–1)	0 (0–0)	0.21
Proximal to culprit frame	0 (0–1)	0 (0–1)	0.44
Distal to culprit frame	0 (0–1)	0 (0–1)	0.45
Spanning culprit frame	0 (0–1)	0 (0–0)	0.07
Distorting	0 (0–1)	0 (0–0)	0.01

Data are presented as median (interquartile range) or mean±SD or n (%). SAP indicates stable angina pectoris; and STEMI-PR, ST-segment–elevation myocardial infarction plaque rupture.

Table 4. Thirty-Millimeter Segment Optical Coherence Tomography Analysis

	STEMI-PR (n=36)	SAP (n=34)	*P* Value
Total calcium deposits	3.5 (2–6)	2 (1–4)	0.08
Spotty calcium	2 (1–4)	1.5 (0–3)	0.06
Large calcium	1 (0–2)	0.5 (0–1)	0.66
Superficial-65	1 (0–2)	0 (0–1.25)	0.60
Superficial-100	1 (0–3)	1 (0–2.25)	0.42
Spotty and superficial-65	0 (0–1)	0 (0–1)	0.72
Spotty and superficial-100	0 (0–1)	0 (0–1.25)	0.59

Data are presented as median (interquartile range). SAP indicates stable angina pectoris; and STEMI-PR, ST-segment–elevation myocardial infarction plaque rupture.

on local plaque vulnerability remains unclear.[13] Computed tomographic studies demonstrated a correlation between a spotty pattern of calcification (<3 mm) and presentation with acute coronary presentations.[14–16] Early pathological studies, however, suggest that although the degree of calcification is an excellent marker for plaque burden, it correlates poorly with luminal narrowing and may not affect the biomechanical stability of atherosclerotic plaques.[17,18]

Intravascular imaging can be performed in vivo to further elucidate the potential role of calcium in plaque vulnerability. In this study, we did not identify a significant difference in the number or pattern of culprit lesion OCT-identified coronary calcium deposits between patients with SAP and STEMI-PR, 2 extremes of clinical presentation. Our findings are in distinct contrast to several IVUS and 1 previous OCT study, which have suggested that spotty and superficial calcium deposits may increase local plaque vulnerability. We think that this difference derives from inherent limitations to IVUS imaging and important methodological dissimilarities between the previous studies and our current investigation.

IVUS Studies of Coronary Artery Calcium

In an early IVUS study by Beckman et al,[19] the relationship between culprit coronary artery calcification and clinical presentation was explored in 78 patients (17 with SAP, 43 with UAP, and 18 with AMI) who had undergone IVUS imaging after stent placement. The maximal arc of calcium within the stented segment and the mean of the calcium arcs measured at the proximal, middle, and distal stented segments increased progressively for the groups of patients with AMI, UAP, then SAP, suggesting that smaller calcium deposits may contribute to unstable clinical presentations. Calcium measurements, however, were only taken from 4 frames within the stented segment, and it is possible that the stented vessel lengths analyzed in this study differed between groups.

A subsequent IVUS study analyzed culprit lesion images obtained before intervention and included 178 patients (47 with SAP, 70 with UAP, and 61 with AMI).[20] The number of spotty calcium deposits was significantly higher in the AMI compared with the SAP group, and the average length of each calcium deposit was smaller in the AMI and UAP groups compared with the SAP group. Calcium analysis was restricted to the 10-mm-long culprit segment (5 mm proximal to 5 mm distal to the culprit lesion frame). The mean number of calcium deposit in the AMI group was 1.4, which is similar to what we found in our study for the STEMI-PR group. The mean number of calcium deposits in the SAP group, however, was 0.5 in the IVUS study, compared with 1.67 in our study. One possible explanation for these discrepant findings is that a single large calcium deposit visualized using IVUS may actually represent multiple smaller calcium deposits that can be distinguished pathologically or with higher-resolution OCT imaging.[8] Figure 2 shows cross-sectional OCT images with multiple calcifications that may seem as a single deposit on lower resolution imaging.

In a study of pooled data from 7 clinical IVUS trials, 1347 patients with stable angina were grouped according to the presence or absence of spotty calcification (arc, <90°). The group with spotty calcification had a greater percent atheroma volume and total atheroma volume at baseline, as well as greater progression of percent atheroma volume on serial evaluation. The authors concluded that spotty calcification was associated with more extensive and diffuse coronary atherosclerosis and accelerated disease progression.[21] Importantly, however,

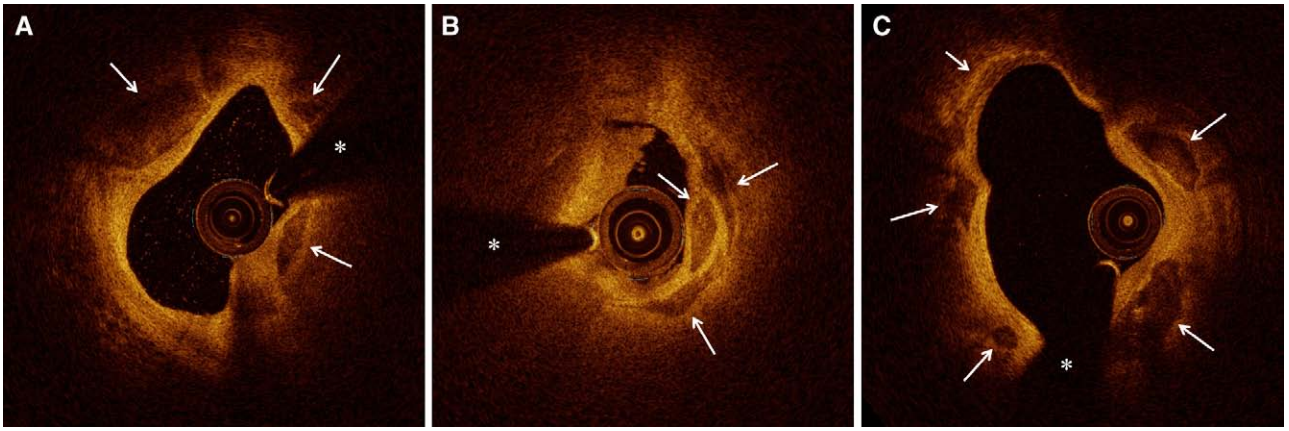

Figure 2. Multiple calcium deposits. **A–C**, The high resolution of optical coherence tomography enables the identification of multiple distinct calcium deposits within single cross-sectional images. The asterisks denote guidewire shadow artifact.

this study evaluated nonculprit vessels, and the study findings may, therefore, not be applicable to the investigation of plaque vulnerability.

Superficial calcifications, in contrast to deep calcifications, have also been implicated in plaque vulnerability. On IVUS imaging, calcium has been defined as superficial if the leading edge of acoustic shadowing seemed within the shallowest 50% of the plaque plus media and deep if it seemed within the deeper 50% of the plaque plus media thickness.[22] A study comparing 101 IVUS-detected ruptured plaques with 101 matched controls found that a significantly larger number of calcium deposits in ruptured versus control plaques; however, this difference was driven by deep calcium deposits, as there was no difference in the number of superficial calcium deposits between groups.[22]

Although IVUS has been shown to be highly sensitive and specific for the identification of calcified plaque, its accuracy in the quantitative assessment of calcium, particularly variability in the measured arc of calcium, has been questioned.[23] In a study using ex vivo coronary arteries, OCT-derived calcium measurements correlated better with histological examination than IVUS-derived measurements.[24] Excellent correlation in the measurement of calcium depth and angle has been shown between OCT-imaged and cryo-imaged cadaveric coronary samples.[25]

OCT Study of Coronary Artery Calcium

To the best of our knowledge, only 1 previous study has used OCT to evaluate the potential role of coronary calcium in plaque vulnerability. In a study of 187 consecutive patients (44 with AMI, 73 with UAP, and 70 with SAP) with coronary artery disease who underwent culprit lesion OCT imaging, Mizukoshi et al[4] found that the arc, length, and area of calcium were significantly smaller in patients presenting with AMI and UAP compared with those presenting with SAP ($P<0.01$). Spotty calcifications with an arc of <90° were significantly more prevalent in the AMI and UAP groups than in the SAP group ($P<0.01$), whereas large calcium deposits with an arc of ≥90° were significantly more prevalent in the SAP group than in the AMI and UAP groups ($P<0.01$). Moreover, the calcifications in the AMI and UAP groups were more superficial than those in the SAP group ($P<0.01$). The authors hypothesized that spotty and superficial calcifications might, therefore, play a role in plaque vulnerability.[4] Importantly, however, a 30-mm segment spanning from 15 mm proximal to 15 mm distal to the culprit site was used for the assessment of plaque morphology. Calcium deposits remote from a culprit rupture site are unlikely to biomechanically contribute to focal risk of rupture, and a previous study suggests that the culprit lesions of patients with acute coronary syndrome are, on average, only ≈16 mm in length.[26] We, therefore, focused our OCT calcium analysis to a 10-mm culprit segment and found no significant difference in the number or pattern of calcium deposits between patients presenting with SAP and STEMI-PR. Interestingly, in the subset of patients in whom culprit lesion OCT images enabled a full 30-mm segment analysis, we found a trend toward a higher number of total and spotty calcium deposits in the STEMI-PR group than in the SAP group, which is consistent with the findings from the study by Mizukoshi et al.[4]

Mathematical Models

Mathematical models investigating the biomechanical effect of calcifications within a fibrous cap support the hypothesis that single microcalcifications[27] and clusters of microcalcifications[28] increase local tissue stress, thereby promoting vulnerability for rupture. These models are frequently cited as supportive evidence for the conclusions drawn by these previous intravascular imaging studies. Importantly, however, the mathematical models emphasize a critical microcalcification size between 5 and 65 μm, outside of which microcalcifications should not be biomechanically dangerous.[29] Calcium deposits of this size are below the resolution of IVUS imaging and challenging to identify on OCT imaging. Although the resolution of OCT imaging is 15 to 20 μm, in our experience, calcium deposits must be several times larger than that to be confidently identified using the defining OCT features of heterogeneous reflectivity with low signal attenuation and a sharply demarcated border. Our findings do not suggest a direct role for OCT-identified coronary calcium, spotty calcium, or superficial calcium in promoting plaque vulnerability for rupture. Rather, as suggested in early pathological studies, coronary calcium may be more reflective of total atherosclerotic risk than local biomechanical instability.

Interestingly, we identified a trend toward a greater number of calcifications spanning the culprit frame and a greater median number of calcium deposits distorting the lumen in patients presenting with SAP than STEMI-PR. One potential explanation for this result is that distorting calcifications occur when calcium deposits form without adequate compensatory positive remodeling. These deposits, therefore, contribute to focal luminal narrowing that, if severe enough, can become a culprit minimum lumen area site that manifests clinically as SAP. Indeed, large plaque burden and small lumen area have been shown to be useful morphological features for discriminating plaques that manifest as culprit lesions from those that remain clinically silent.[30]

Limitations

There are several limitations to our study that merit acknowledgment. First, the study population was small, including 108 patients totally (55 with SAP and 53 with STEMI-PR). Second, OCT imaging was performed at the discretion of the operator, introducing potential selection bias. Third, the differentiation of lipid pools from calcium deposits on OCT imaging can be challenging. However, the sharply demarcated border of calcium, in comparison with the scattered border of lipid, has been used as an important distinguishing characteristic.[31] In addition, algorithms are under development for more objective and automated OCT-identification of calcium.[32,33] Fourth, residual thrombus, particularly in the STEMI-PR group, may have limited the identification of underlying calcium deposits. We, therefore, excluded cases with poor OCT image quality, including cases with excessive residual thrombus. It is possible that specific patterns of

plaque calcification may be associated with greater thrombogenicity, and the exclusion of these cases may, therefore, have influenced our results.

Conclusions

In contrast to previous IVUS and OCT studies, we found no significant difference in the number or pattern of culprit segment calcium deposits between patients presenting with SAP and STEMI-PR. This discrepancy may be derived from the limited resolution of IVUS imaging and important methodological differences between this and previous intravascular imaging studies. Coronary calcification, as assessed by OCT, may not be a useful marker of local plaque vulnerability as previously suspected.

Disclosures

Dr Jang received a research grant and honorarium from St. Jude Medical, and his research was also supported by Michael Park and Kathryn Park and by Allan Gray and Gillian Gray. The other authors report no conflicts.

References

1. Rumberger JA, Simons DB, Fitzpatrick LA, Sheedy PF, Schwartz RS. Coronary artery calcium area by electron-beam computed tomography and coronary atherosclerotic plaque area. A histopathologic correlative study. *Circulation*. 1995;92:2157–2162.
2. Arad Y, Spadaro LA, Goodman K, Newstein D, Guerci AD. Prediction of coronary events with electron beam computed tomography. *J Am Coll Cardiol*. 2000;36:1253–1260.
3. Ehara S, Kobayashi Y, Yoshiyama M, Ueda M, Yoshikawa J. Coronary artery calcification revisited. *J Atheroscler Thromb*. 2006;13:31–37.
4. Mizukoshi M, Kubo T, Takarada S, Kitabata H, Ino Y, Tanimoto T, Komukai K, Tanaka A, Imanishi T, Akasaka T. Coronary superficial and spotty calcium deposits in culprit coronary lesions of acute coronary syndrome as determined by optical coherence tomography. *Am J Cardiol*. 2013;112:34–40. doi: 10.1016/j.amjcard.2013.02.048.
5. Cardoso L, Weinbaum S. Changing views of the biomechanics of vulnerable plaque rupture: a review. *Ann Biomed Eng*. 2014;42:415–431. doi: 10.1007/s10439-013-0855-x.
6. Abedin M, Tintut Y, Demer LL. Vascular calcification: mechanisms and clinical ramifications. *Arterioscler Thromb Vasc Biol*. 2004;24:1161–1170. doi: 10.1161/01.ATV.0000133194.94939.42.
7. Henein M, Granåsen G, Wiklund U, Schmermund A, Guerci A, Erbel R, Raggi P. High dose and long-term statin therapy accelerate coronary artery calcification. *Int J Cardiol*. 2015;184:581–586. doi: 10.1016/j.ijcard.2015.02.072.
8. Mintz GS. Intravascular imaging of coronary calcification and its clinical implications. *JACC Cardiovasc Imaging*. 2015;8:461–471. doi: 10.1016/j.jcmg.2015.02.003.
9. Jang IK, Bouma BE, Kang DH, Park SJ, Park SW, Seung KB, Choi KB, Shishkov M, Schlendorf K, Pomerantsev E, Houser SL, Aretz HT, Tearney GJ. Visualization of coronary atherosclerotic plaques in patients using optical coherence tomography: comparison with intravascular ultrasound. *J Am Coll Cardiol*. 2002;39:604–609.
10. Kataoka Y, Puri R, Hammadah M, Duggal B, Uno K, Kapadia SR, Tuzcu EM, Nissen SE, Nicholls SJ. Spotty calcification and plaque vulnerability in vivo: frequency-domain optical coherence tomography analysis. *Cardiovasc Diagn Ther*. 2014;4:460–469. doi: 10.3978/j.issn.2223-3652.2014.11.06.
11. Tearney GJ, Regar E, Akasaka T, Adriaenssens T, Barlis P, Bezerra HG, Bouma B, Bruining N, Cho JM, Chowdhary S, Costa MA, de Silva R, Dijkstra J, Di Mario C, Dudek D, Dudeck D, Falk E, Falk E, Feldman MD, Fitzgerald P, Garcia-Garcia HM, Garcia H, Gonzalo N, Granada JF, Guagliumi G, Holm NR, Honda Y, Ikeno F, Kawasaki M, Kochman J, Koltowski L, Kubo T, Kume T, Kyono H, Lam CC, Lamouche G, Lee DP, Leon MB, Maehara A, Manfrini O, Mintz GS, Mizuno K, Morel MA, Nadkarni S, Okura H, Otake H, Pietrasik A, Prati F, Räber L, Radu MD, Rieber J, Riga M, Rollins A, Rosenberg M, Sirbu V, Serruys PW, Shimada K, Shinke T, Shite J, Siegel E, Sonoda S, Sonada S, Suter M, Takarada S, Tanaka A, Terashima M, Thim T, Troels T, Uemura S, Ughi GJ, van Beusekom HM, van der Steen AF, van Es GA, van Es GA, van Soest G, Virmani R, Waxman S, Weissman NJ, Weisz G; International Working Group for Intravascular Optical Coherence Tomography (IWG-IVOCT). Consensus standards for acquisition, measurement, and reporting of intravascular optical coherence tomography studies: a report from the International Working Group for Intravascular Optical Coherence Tomography Standardization and Validation. *J Am Coll Cardiol*. 2012;59:1058–1072. doi: 10.1016/j.jacc.2011.09.079.
12. Stary HC. The development of calcium deposits in atherosclerotic lesions and their persistence after lipid regression. *Am J Cardiol*. 2001;88(2A):16E–19E.
13. Alexopoulos D, Moulias A. In the search of coronary calcium. *Int J Cardiol*. 2013;167:310–317. doi: 10.1016/j.ijcard.2012.06.051.
14. Motoyama S, Kondo T, Sarai M, Sugiura A, Harigaya H, Sato T, Inoue K, Okumura M, Ishii J, Anno H, Virmani R, Ozaki Y, Hishida H, Narula J. Multislice computed tomographic characteristics of coronary lesions in acute coronary syndromes. *J Am Coll Cardiol*. 2007;50:319–326. doi: 10.1016/j.jacc.2007.03.044.
15. Kim SY, Kim KS, Seung MJ, Chung JW, Kim JH, Mun SH, Lee YS, Lee JB, Ryu JK, Choi JY, Chang SG. The culprit lesion score on multi-detector computed tomography can detect vulnerable coronary artery plaque. *Int J Cardiovasc Imaging*. 2010;26(suppl 2):245–252. doi: 10.1007/s10554-010-9712-2.
16. Puchner SB, Liu T, Mayrhofer T, Truong QA, Lee H, Fleg JL, Nagurney JT, Udelson JE, Hoffmann U, Ferencik M. High-risk plaque detected on coronary CT angiography predicts acute coronary syndromes independent of significant stenosis in acute chest pain: results from the ROMICAT-II trial. *J Am Coll Cardiol*. 2014;64:684–692. doi: 10.1016/j.jacc.2014.05.039.
17. Burke AP, Weber DK, Kolodgie FD, Farb A, Taylor AJ, Virmani R. Pathophysiology of calcium deposition in coronary arteries. *Herz*. 2001;26:239–244.
18. Huang H, Virmani R, Younis H, Burke AP, Kamm RD, Lee RT. The impact of calcification on the biomechanical stability of atherosclerotic plaques. *Circulation*. 2001;103:1051–1056.
19. Beckman JA, Ganz J, Creager MA, Ganz P, Kinlay S. Relationship of clinical presentation and calcification of culprit coronary artery stenoses. *Arterioscler Thromb Vasc Biol*. 2001;21:1618–1622.
20. Ehara S, Kobayashi Y, Yoshiyama M, Shimada K, Shimada Y, Fukuda D, Nakamura Y, Yamashita H, Yamagishi H, Takeuchi K, Naruko T, Haze K, Becker AE, Yoshikawa J, Ueda M. Spotty calcification typifies the culprit plaque in patients with acute myocardial infarction: an intravascular ultrasound study. *Circulation*. 2004;110:3424–3429. doi: 10.1161/01.CIR.0000148131.41425.E9.
21. Kataoka Y, Wolski K, Uno K, Puri R, Tuzcu EM, Nissen SE, Nicholls SJ. Spotty calcification as a marker of accelerated progression of coronary atherosclerosis: insights from serial intravascular ultrasound. *J Am Coll Cardiol*. 2012;59:1592–1597. doi: 10.1016/j.jacc.2012.03.012.
22. Fujii K, Carlier SG, Mintz GS, Takebayashi H, Yasuda T, Costa RA, Moussa I, Dangas G, Mehran R, Lansky AJ, Kreps EM, Collins M, Stone GW, Moses JW, Leon MB. Intravascular ultrasound study of patterns of calcium in ruptured coronary plaques. *Am J Cardiol*. 2005;96:352–357. doi: 10.1016/j.amjcard.2005.03.074.
23. Kostamaa H, Donovan J, Kasaoka S, Tobis J, Fitzpatrick L. Calcified plaque cross-sectional area in human arteries: correlation between intravascular ultrasound and undecalcified histology. *Am Heart J*. 1999;137:482–488.
24. Kume T, Okura H, Kawamoto T, Yamada R, Miyamoto Y, Hayashida A, Watanabe N, Neishi Y, Sadahira Y, Akasaka T, Yoshida K. Assessment of the coronary calcification by optical coherence tomography. *EuroIntervention*. 2011;6:768–772. doi: 10.4244/EIJV6I6A130.
25. Mehanna E, Bezerra HG, Prabhu D, Brandt E, Chamié D, Yamamoto H, Attizzani GF, Tahara S, Van Ditzhuijzen N, Fujino Y, Kanaya T, Stefano G, Wang W, Gargesha M, Wilson D, Costa MA. Volumetric characterization of human coronary calcification by frequency-domain optical coherence tomography. *Circ J*. 2013;77:2334–2340.
26. Jia H, Abtahian F, Aguirre AD, Lee S, Chia S, Lowe H, Kato K, Yonetsu T, Vergallo R, Hu S, Tian J, Lee H, Park SJ, Jang YS, Raffel OC, Mizuno K, Uemura S, Itoh T, Kakuta T, Choi SY, Dauerman HL, Prasad A, Toma C, McNulty I, Zhang S, Yu B, Fuster V, Narula J, Virmani R, Jang IK. In vivo diagnosis of plaque erosion and calcified nodule in patients with acute coronary syndrome by intravascular optical coherence tomography. *J Am Coll Cardiol*. 2013;62:1748–1758. doi: 10.1016/j.jacc.2013.05.071.
27. Vengrenyuk Y, Carlier S, Xanthos S, Cardoso L, Ganatos P, Virmani R, Einav S, Gilchrist L, Weinbaum S. A hypothesis for vulnerable plaque

rupture due to stress-induced debonding around cellular microcalcifications in thin fibrous caps. *Proc Natl Acad Sci U S A*. 2006;103:14678–14683. doi: 10.1073/pnas.0606310103.
28. Maldonado N, Kelly-Arnold A, Vengrenyuk Y, Laudier D, Fallon JT, Virmani R, Cardoso L, Weinbaum S. A mechanistic analysis of the role of microcalcifications in atherosclerotic plaque stability: potential implications for plaque rupture. *Am J Physiol Heart Circ Physiol*. 2012;303:H619–H628. doi: 10.1152/ajpheart.00036.2012.
29. Maldonado N, Kelly-Arnold A, Cardoso L, Weinbaum S. The explosive growth of small voids in vulnerable cap rupture; cavitation and interfacial debonding. *J Biomech*. 2013;46:396–401. doi: 10.1016/j.jbiomech.2012.10.040.
30. Tian J, Ren X, Vergallo R, Xing L, Yu H, Jia H, Soeda T, McNulty I, Hu S, Lee H, Yu B, Jang IK. Distinct morphological features of ruptured culprit plaque for acute coronary events compared to those with silent rupture and thin-cap fibroatheroma: a combined optical coherence tomography and intravascular ultrasound study. *J Am Coll Cardiol*. 2014;63:2209–2216. doi: 10.1016/j.jacc.2014.01.061.
31. Manfrini O, Mont E, Leone O, Arbustini E, Eusebi V, Virmani R, Bugiardini R. Sources of error and interpretation of plaque morphology by optical coherence tomography. *Am J Cardiol*. 2006;98:156–159. doi: 10.1016/j.amjcard.2006.01.097.
32. Wang Z, Kyono H, Bezerra HG, Wang H, Gargesha M, Alraies C, Xu C, Schmitt JM, Wilson DL, Costa MA, Rollins AM. Semiautomatic segmentation and quantification of calcified plaques in intracoronary optical coherence tomography images. *J Biomed Opt*. 2010;15:061711. doi: 10.1117/1.3506212.
33. Celi S, Vaghetti M, Palmieri C, Berti S. Superficial coronary calcium analysis by OCT: looking forward an imaging algorithm for an automatic 3D quantification. *Int J Cardiol*. 2013;168:2958–2960. doi: 10.1016/j.ijcard.2013.03.115.

CLINICAL PERSPECTIVE

Despite improvements in stent technology, implantation techniques, and adjunctive medical therapy, the risk of recurrent cardiac events after successful percutaneous coronary intervention remains high. The identification of vulnerable plaques at high risk for evolving into culprit plaques, therefore, remains an active area of investigation. Intravascular imaging has facilitated the identification of multiple morphological features associated with plaque vulnerability, and previous studies have suggested that spotty superficial calcium deposits may be a marker of increased plaque vulnerability. These studies, however, had methodological limitations. In this study, we performed a detailed assessment of culprit lesion coronary calcification using optical coherence tomography. We found no significant difference in the number or pattern of calcium deposits between patients who presented with ST-segment–elevation myocardial infarction mediated by plaque rupture versus patients who presented with stable angina. Our findings suggest that coronary calcification, as assessed using optical coherence tomography, may not be a useful marker of local plaque vulnerability as previously suspected.